Cryogenic pulsed inductive microwave magnetometer

A. B. Kos,[a] J. P. Nibarger, R. Lopusnik, T. J. Silva, and Z. Celinski
National Institute of Standards and Technology, Magnetic Technology Division, 325 Broadway, Boulder, Colorado 80305

(Presented on 13 November 2002)

A cryogenic pulsed inductive microwave magnetometer is used to characterize the switching dynamics in thin-film magnetic materials at low temperatures and microwave frequencies. The system is contained inside a 20-cm-diam ultrahigh vacuum chamber and cooled by a cryopump that allows measurements between 20 and 350 K. A temperature controller regulates the sample temperature using two silicon diodes as sensors. Applied magnetic fields of up to 36 kA/m (450 Oe) are generated by a four-pole, water-cooled electromagnet with independent control of each axis. Magnetic switching in the sample is driven by high-speed current step pulses in a coplanar waveguide structure with the sample placed in a flip-chip configuration. A 20 GHz sampling oscilloscope is used to record the dynamics of the magnetic reorientation. The switching dynamics are given for a 10-nm-thick Ni–Fe film at 30 K in response to a 1 kA/m field step.
[DOI: 10.1063/1.1543125]

I. INTRODUCTION

The theoretical understanding of magnetic damping in ferromagnetic transition metals was strongly influenced by the observation of temperature dependent damping in ferromagnetic resonance (FMR) measurements.[1] For pure bulk Ni, and to a lesser extent for hcp Co, the damping increases significantly for temperatures below 100 K.[2] This was understood in terms of magnon-electron scattering effects, wherein two physical processes conspire to drive the damping process: (1) spin-orbit coupling mixes spin states of the conduction electrons and (2) the Fermi surface is deformed by the spin wave excitations.[3,4] The combined effect of such band mixing and Fermi surface deformation manifests itself as a dependence of the magnon relaxation rate on the electron mean free path.[5] It has been argued that the observation of an intrinsic (i.e., NOT based on inhomogeneous line broadening effects, but all other loss mechanisms that take energy out of the spin system) Gilbert damping parameter is a further signature of ubiquitous magnon-electron scattering in conducting ferromagnets. More specifically, the determination of a slope for field-swept linewidth versus frequency from a FMR measurement is consistent with a *confluence* mechanism for damping, of which magnon-electron scattering is one particular case.[6]

However, in spite of this considerable theoretical framework, it is not yet known to what extent magnon-electron scattering is applicable in the case of magnetic switching, where both the range and frequency of the angular motion are significantly different than in the case of FMR. To answer this and other questions, experimental methods are required to determine whether similar temperature dependences exist for the damping of gyromagnetic motion under sudden reorientation of the equilibrium direction of magnetization.

The aim of this article is to describe in detail the development of a cryogenic pulsed inductive microwave magnetometer (CryoPIMM). The instrument is based upon a previously described room-temperature form of the magnetometer that employs the inductive coupling between a magnetic sample and a high-bandwidth waveguide to perform high-speed measurements of magnetic switching dynamics in thin-film samples.[7,8] We discuss the components and assembly of the system as well as the procedures necessary to make measurements. In addition, we present preliminary measurements on Ni–Fe films at 30 K to illustrate the cryogenic performance of the system.

The CryoPIMM can make pulsed-field magnetodynamic measurements of thin-film samples over a temperature range of 20–325 K. Material parameters that can be extracted from these measurements include anisotropy, Landé g factor, and damping parameter α, as well as the permeability as a function of frequency. The system uses a coplanar waveguide to supply high-speed field pulses to the magnetic film; it also serves as an inductive flux sensor. A 10 V pulse generator produces 45 ps rise time step wave forms with 10 ns duration to drive the sample dynamics. A sampling oscilloscope with a 20 GHz bandwidth captures the inductive response. Software automatically coordinates control and data acquisition, including application of static external fields, temperature control, pulse parameter adjustment, and data postprocessing.

A complete system that incorporated magnetic field and microwave sources into a vacuum chamber was assembled to perform microwave magnetic measurements at cryogenic temperatures. Figure 1 shows the system, based on a 20.3-cm-diam, 20.3-cm-high vacuum chamber that has two 25 cm and eight 7 cm copper gasket-sealed flanges. A cryopump is attached to the bottom 25 cm flange while the top flange is used as a loading port. The eight 7 cm flanges are used as instrumentation and utility ports. The system is evacuated using a turbo-molecular pump that can reach pressures less

[a]Author to whom correspondence should be addressed: electronic mail: kos@boulder.nist.gov.

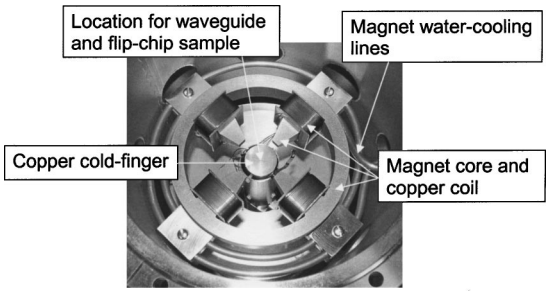

FIG. 1. Photo of inside of cryostat (with waveguide removed).

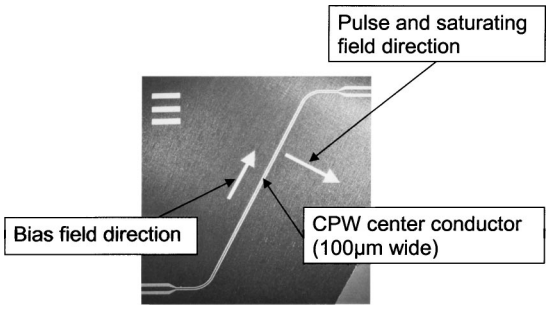

FIG. 2. Photo of coplanar waveguide indicating direction of applied magnetic fields. The sample is laid directly onto the waveguide with a submicrometer layer of photoresist on the metallic magnetic layer to prevent shorting of the coplanar center conductor. The 60° bends in the CPW accommodate the restricted space available between the pole pieces of the bias magnet structure.

than 0.13 Pa (1 mTorr) in approximately 10 min.

A cryopump is employed in conjunction with a closed-cycle helium compressor to cool the sample. The refrigerator is able to achieve 20 K despite thermal loading by the copper coaxial cables, with the added benefit of being able to remain at constant temperature indefinitely. The sample is placed on a pure copper cold finger (2.5 cm diameter, 15 cm length) that is mounted onto the cooling stage of the cryopump. Such a large thermal mass improves the long-term temperature stability. An additional stainless steel radiation shield is mounted around the cold finger and maintained at a temperature of 80 K. A temperature controller regulates the sample temperature using two silicon diodes as sensors, one mounted on the cold finger 1 mm below the sample surface, and the other mounted onto the coplanar waveguide assembly.

The CryoPIMM system requires two mutually perpendicular static magnetic field sources to perform the measurement. To achieve sufficiently high magnetic field strengths we designed an electromagnet with two sets of soft iron pole pieces and circular yoke as shown in Fig. 1. The coils are wound using square magnet wire with heavy insulation (rated at 513 K) onto rectangular copper coil forms. The magnets must be cooled to keep the system from overheating when fully energized in vacuum. This is accomplished with a regulated water chiller connected to the coil forms by copper tubing and clamps that are attached directly to the coil forms. The cooling system significantly reduced both the resistivity drift in the magnets and outgassing of the coils at high fields. The design of the magnet was iteratively modeled using finite element software to reduce the effect of flux shunting between the two perpendicular directions and maximize the field strength. Field uniformity along the waveguide is better than 1% over a length of 4 mm. The gap width between the pole faces is 35 mm. The resistance of each coil pair is approximately 0.8 Ω when connected in series at room temperature, permitting fields of up to 36 kA/m (450 Oe) when used with two 12 A, 10 V current supplies.

The coplanar waveguide (CPW) design was constrained by three stringent engineering requirements: (1) The CPW must have an extremely high bandwidth in excess of 8 GHz, sufficient to detect FMR signals in high moment materials at fields of up to 36 kA/m. (2) The CPW must be free of any ferrous materials with Curie temperatures below room temperature that might generate spurious inductive signals. (3) The CPW must fit between the magnet pole faces, yet still provide a straight waveguide section greater than 2 cm in length in order to accommodate large sample substrates. While the flux sensing section of the CPW must be oriented rectilinear to the applied magnetic field axes, the interconnecting coaxial cable must come in at an angle with respect to the field direction due to the presence of the pole faces. This required that two gradual (60°) turns be incorporated into the CPW structure (see Fig. 2). The CPW was constructed using 1.3-mm-thick Duroid[9] with 17-μm-thick Cu cladding. The center conductor width was 100 μm with a gap width of 100 μm. Standard photolithography techniques and chemical etching were used to fabricate the waveguide structure.

A rigid copper coaxial cable (2.16 mm outer diameter, 0.51 mm center conductor diameter) was soldered directly to the waveguide to make a strong, reliable, nonmagnetic contact to the CPW. A 2 mm section of the waveguide was removed, the coax was inserted, and the ground planes were soldered into place. The center conductor of the waveguide (100 μm width) was tapered to a larger width to mate with the larger coax center conductor, which was likewise machined into a smaller taper. The two conductors were carefully soldered together. All soldering was done under a microscope and all parts were clamped in place while soldering to prevent movement of the conductors relative to each other due to heat-induced expansion of the coax dielectric. The waveguide/coax assembly was mounted onto a brass holder, which clamps the rigid coax and waveguide securely, to prevent damage while being installed onto the cryopump cold finger. The CPW characteristic impedance was measured to be $50 \pm 0.5\,\Omega$ using time-domain reflectometry; the 3 dB bandwidth was 12 GHz, as obtained with a vector network analyzer.

We use a pulse generator that produces a 10 V step with a rise time of 45 ps to generate the fast field step transition. The magnetic field generated directly over the center conductor of the CPW is estimated to be 1 kA/m (13 Oe), using the Biot–Savart law and assuming a uniform current distribution in the CPW center conductor. To maximize the field at the sample, a layer of photoresist less than 1 μm thick is spin coated onto the ferromagnetic film. The sample is then placed in contact with the waveguide, with the photoresist preventing any shorting of the waveguide by the film. The

timing jitter of the pulse generator is less than 1.5 ps rms. A 20 GHz sampling oscilloscope records the voltage induced into the waveguide by the sample when it switches. To increase the signal-to-noise ratio we perform multiple averages of two oscilloscope traces: one in which the sample magnetization is allowed to rotate freely under the influence of the pulsed field, and one with the sample fully saturated (by an externally applied static magnetic field) in the same direction as the pulsed field.[7]

The system software records data as a function of bias field and temperature. After setting the temperature and waiting for it to stabilize, the software applies the appropriate fields and records the two traces, as described above, as a function of bias field strength. These data are then postprocessed, which involves subtracting the two voltage wave forms, integrating the subtracted wave form to obtain the flux, performing a fast Fourier transform to determine the frequency dependence, and plotting the precessional frequency versus bias field. The system software and measurement procedures are identical to that used in the previous PIMM version[8] with the addition of automatic temperature control.

II. EXPERIMENT AND RESULTS

To illustrate the performance of the system we present measurements for a 10-nm-thick $Ni_{81}Fe_{19}$ film grown on a glass substrate by dc magnetron sputtering in an Ar atmosphere at 0.53 Pa (4 mTorr) with an initial 5 nm Ta adhesion layer. The base pressure in the deposition chamber was 1.33×10^{-6} Pa (10^{-8} Torr). Figure 3 shows an example of the time-domain response at 30 and 250 K. A magnetic bias field of 2.8 kA/m (35 Oe) was applied along the easy axis for these measurements. The curves show a typical Ni–Fe response, with a pronounced overshoot and underdamped oscillatory ringing. However, the duration of the oscillatory ringing is significantly longer at the higher temperature. In addition, the frequency of the precessional oscillations was markedly lower at the higher temperature: 2.07 GHz at $T=250$ K, and 2.98 GHz at $T=30$ K. Frequency-domain analysis was used to determine the characteristic frequency. The Gilbert damping parameter α was extracted from frequency-domain analysis: $\alpha=0.0097$ at $T=250$ K and $\alpha=0.0291$ at $T=30$ K.

The strong increase in damping at low temperatures is suggestive of magnon-electron scattering effects. However, the decrease in permeability at low temperatures is not expected. The commensurate increase in precessional frequency suggests that the decrease in the permeability (shown as a decrease in flux from roughly 1.2 pWb at 250 K to 0.5 pWb at 30 K) is the result of an increase in the effective anisotropy of the material, rather than any decrease in the net magnetic moment. Further investigation is required to determine whether the increase in damping can be attributed to variations in the electron mean free path, or whether the effect is correlated with the increase in the apparent anisotropy.

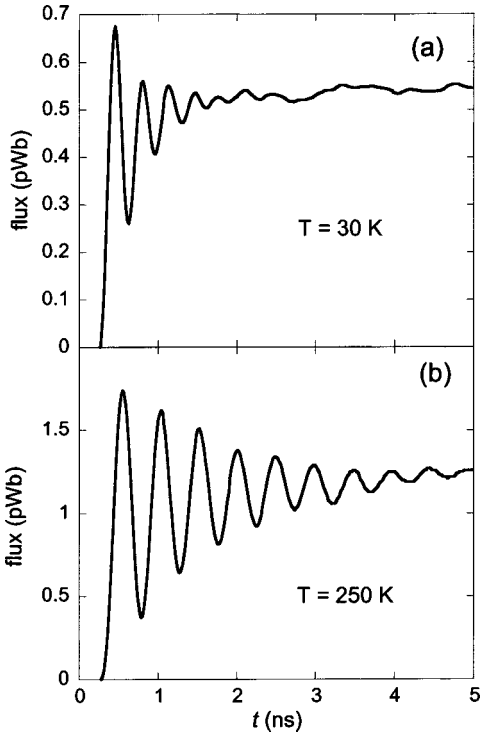

FIG. 3. Integrated time-domain response of a 10 nm $Ni_{81}Fe_{19}$ film measured with the CryoPIMM at (a) $T=30$ K and (b) $T=250$ K. The sample was saturated along the easy axis with a magnetic bias field of 2.8 kA/m (35 Oe). The precessional response at the lower temperature indicates a higher resonant frequency, reduced permeability, and greater damping.

[1] S. M. Bhagat and L. L. Hirst, Phys. Rev. **151**, 401 (1966).
[2] S. M. Bhagat and P. Lubitz, Phys. Rev. B **10**, 179 (1974).
[3] B. Heinrich, D. Fraitova, and V. Kambersky, Phys. Status Solidi **23**, 501 (1967).
[4] V. Korenmann and R. E. Prange, Phys. Rev. B **6**, 2679 (1972).
[5] B. Heinrich, D. J. Meredith, and J. F. Cochran, J. Appl. Phys. **50**, 7726 (1979).
[6] V. Kambersky and C. E. Patton, Phys. Rev. B **11**, 2668 (1975).
[7] T. J. Silva, C. S. Lee, T. M. Crawford, and C. T. Rogers, J. Appl. Phys. **85**, 7849 (1999).
[8] A. B. Kos, T. J. Silva, and P. Kabos, Rev. Sci. Instrum. **73**, 3563 (2002).
[9] Duroid is a registered trademark of the Rogers Corporation. Certain commercial materials are identified to specify the experimental study adequately. This does not imply endorsement by the National Institute of Standards and Technology or that the materials are the best available for the purpose.